MATHEMATICAL METHOD IN ELECTROMAGNETIC THEORY

Splitting of Super-Broadband Pulses by Simple Inhomogeneities of Circular and Coaxial Waveguides

K.Yu. Sirenko

A. Usikov Institute of Radio Physics and Electronics,
National Academy of Sciences of Ukraine
12, Academician Proskura St., Kharkiv 61085, Ukraine

ABSTRACT: The electrodynamic characteristics of simple inhomogeneities in multimode circular and coaxial waveguides are considered in the paper. The phenomena of mode and frequency-mode layering of ultra-wideband signals by stepwise or smooth couplings of waveguides of different cross-sections and by cone-shaped dead pieces in circular and coaxial waveguides have been revealed and studied.

INTRODUCTION

The mode transforming properties of dualport, axially symmetric waveguiding structures were analyzed in detail by frequency domain methods in papers [1-3]. The writers considered structure geometries specified by simple coordinate-related boundaries, and frequency ranges corresponding to single- to three-wave operation modes of waveguide transformers. The full transmission and total reflection effect of monochromatic waves were revealed and investigated for semi-transparent structures. Bandstop and bandpass filters, as well as simple resonant absorbers with low contrast dielectric insertions and other devices were synthesized, based on inhomogeneities of circular waveguides with evanescent modes.

The present paper suggests new physical results. They have been obtained within the rigorous time-domain methods based on the construction of the so-called exact absorbing conditions [4] and inclusion of these into the standard computational scheme of the finite difference technique.

All the physical units used in the paper correspond to the SI, except that the temporal variable t represents a product of the real time and the velocity of light

in a vacuum. The dimensions are suppressed in the body of the paper. The notation used in the problems under analysis is as follows: $k = 2\pi / \lambda$ is the wavenumber (frequency parameter or simply the frequency), with λ being the free space wavelength; ρ, ϕ and z are a polar cylindrical frame whose axis of symmetry coincides with the z -axis $\left(\partial / \partial \phi \equiv 0 \right)$; $\vec{E} \equiv \vec{E}(g,t) = \left\{ E_\rho, E_\phi, E_z \right\}$ and $\vec{H} \equiv \vec{H}(\rho,t) = \left\{ H_\rho, H_\phi, H_z \right\}$ are the electric and magnetic field vectors, respectively; $g = \left\{ \rho, z \right\}$ is a point in the 2D-space; $\mathbf{L} = \mathbf{L}_1 \bigcup \mathbf{L}_2 \bigcup ... \bigcup \mathbf{L}_N$ are virtual boundaries of the waveguide transformer $\mathbf{Q}_L$; N is the number of channels (regular waveguides)through which propagate the signals $U^i(g,t)$ that excite the range $\mathbf{Q}_L$, and $U(g,t)$ that are formed by the section; $v_n^\phi(z,t)$ and $v_n^\rho(z,t)$ ($u_n^\phi(z,t)$ and $u_n^\rho(z,t)$) are space-and-time amplitudes of the field components of the pulsed waves $U^i(g,t)$ $\left(U(g,t) \right)$; $W_{np}^{jq}(k)$ is the fraction of energy carried by mode n of waveguide j when the structure is excited by mode p from waveguide q; k_{nj} is the mode n cut-off frequency in waveguide j , and $T_{np}^{jq}(k)$ are conversion coefficients of mode n in waveguide j into mode p of waveguide q (or transmission factors).

The spectral characteristics $\tilde{f}(k)$ are obtained from the temporal ones, $f(t)$, using the integral Fourier transformation,

$$\tilde{f}(k) = \frac{1}{2\pi} \int_0^T f(t) e^{ikt} dt \quad \leftrightarrow \quad f(t) = \int_{-\infty}^{\infty} \tilde{f}(k) e^{-ikt} dk \qquad (1)$$

(image $\leftrightarrow$ original; T is the upper limit of the observation time interval t). The geometrical parameters of the model problems under consideration were specified in meters. However, all the results obtained can be easily recalculated for any other structures of similar geometry.

STEP-LIKE AND TAPERED JUNCTIONS: MODE SPLITTING OF SUPER-BROADBAND SIGNALS

The step junction of waveguides of differing transverse sized (see Fig. 1(a)) represents the simplest signal transforming inhomogeneity. The appropriate frequency response has been analyzed in [1]. Also noted in the nook are some

effects of particular interest for the design of mode converter devices. These are related to the specific behavior shown by the transmission factors $T_{np}^{21}(k)$. One is that the $\left|T_{np}^{21}(k)\right|$ dependences for k's greatly exceeding k_{n2} attain a practically constant level which is determined by the value $\theta = a_1/a_2$ alone. The latter represents the ratio of the radius of the narrower waveguide (w1) to that of the wider waveguide (w2).
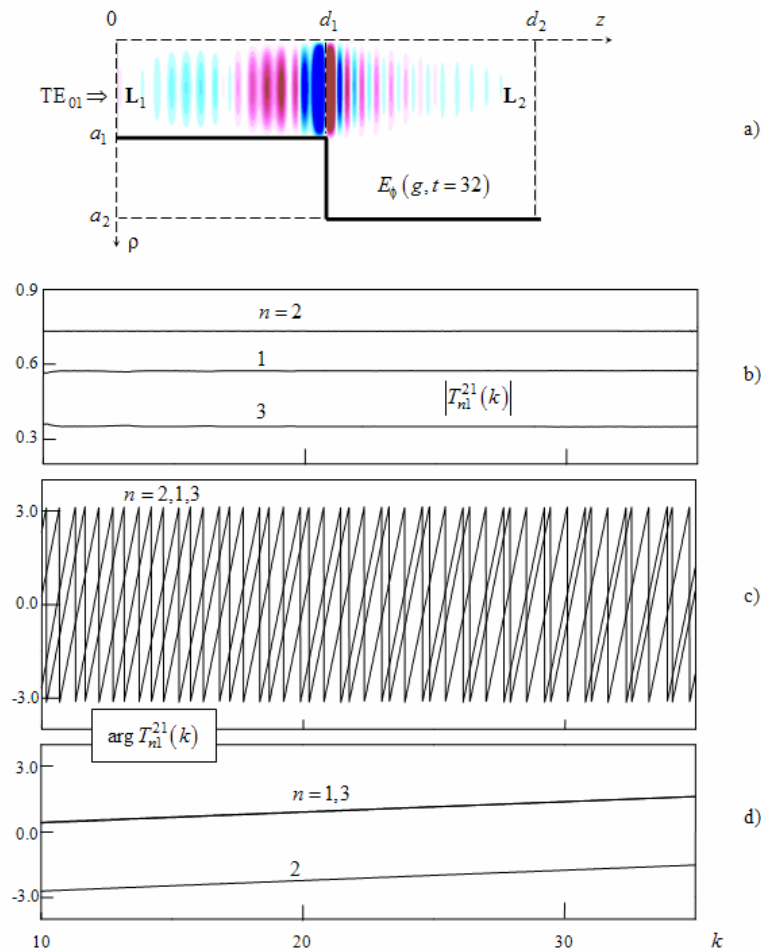
FIGURE 1. Geometry of the step junction and spatial distribution of the $E_\phi(g,t)$ magnitudes for moment when the main body of the pulse crosses the jump in circular waveguide cross-section ((a) $a_1 = 1$, $a_2 = 1.83$, $d_1 = 2$, $d_2 = 4$; the axis of symmetry of the structure coincides with the z-axis). Absolute values (b) and arguments (c) of the transmission factors $T_{n1}^{21}(k)$, for the first three TE_{0n}-modes of the wider waveguide. Phase characteristics of the junction with short arms (d).

Let a TE_{01} pulse, $U^i(g,t)$, with the H_ρ-field component amplitude equal to

$$v_1^\rho(0,t) = 4\frac{\sin\left(\Delta k\left(t-\tilde{T}\right)\right)}{\left(t-\tilde{T}\right)}\cos\left(\tilde{k}\left(t-\tilde{T}\right)\right)\chi(T-t) = F_1(t)$$

be incident on a step junction whose geometry is shown in Fig. 1(a). The control frequency of the signal is $\tilde{k} = 20$. The parameters $\Delta k = 16$, $\tilde{T} = 30$ and $T = 120$ characterize its spectral width, delay time (the time moment at which the main body of the pulse crosses the boundary $\mathbf{L}_1$) and duration ($\chi(...)$ is the Heaviside step function). Within the range $4.5 < k < 35.5$ the spectral amplitudes of the H_ρ field component of this wave (or, briefly, of $U^i(g,t)$, i.e., $v_1^\rho(0,t) = F_1(t)$; $\tilde{k} = 20$, $\Delta k = 16$, $\tilde{T} = 30$ and $T = 120$) differ but slightly from one. The left-hand (narrower) waveguide is a single mode (1-M) structure at the beginning of this range ($k < 7.01$) while an 11-M guide at the end ($k > 35.34$). The right-hand (broader) arm is a 2-M waveguide at ($k < 5.55$) to become 20-M at the end of the range, ($k > 34.76$). The value $\theta = a_1/a_2 = 0.546$ is such that the propagation constants are equal for the first mode in the waveguide w1 and the second mode in w2. In other words, conditions exist which favor a strong mutual conversion of these waves [1]. The coefficients $\left|T_{n1}^{21}(k)\right| = \left|\tilde{u}_n^\phi(d_2,k)/\tilde{v}_1^\phi(0,k)\right|$ are practically constant for the essential transmitted waves, provided that the magnitudes of k are noticeably in excess of k_{n2} (see Fig. 1(b) where $k_{12} \approx 2.09$, $k_{22} \approx 3.83$ and $k_{32} \approx 5.56$). As could expected, the contribution of the second mode, to the wave field in the wider waveguide is predominant. The mode carries about 54% of the power fed in.

Within the range of great k's the behavior shown by phase characteristics of the basic modes propagating in the wider waveguide is determined by the relation $\arg T_{n1}^{21}(k) = \arg\tilde{u}_n^\phi(d_2,k) - \arg\tilde{v}_1^\phi(0,k) \approx d_2\cdot k + A_n$ (see Fig. 1(c) and 1(d)). Hence, in the case of $U^i(g,t)$ whose spectral components are concentrated within the frequency band $K_1 < k < K_2$; $K_1 \gg k_{n2}$, the time-domain amplitudes $u_n^\phi(d_2,t+d_2)$ of the transmitted pulsed waves should reproduce at the boundary $\mathbf{L}_2$ the time-domain amplitude $v_1^\phi(0,t)$ of the

primary wave, although with slight distortions of the waveform and apart from a constant factor. Indeed, according to Eq. (1) we have

$$u_n^\phi\left(d_2, t+d_2\right) = \int\limits_{-\infty}^{\infty} \tilde{u}_n^\phi\left(d_2, k\right) e^{-ik(t+d_2)} dk =$$

$$= \int\limits_{-\infty}^{\infty} \left|T_{n1}^{21}\left(k\right)\right| \tilde{v}_1^\phi\left(0, k\right) e^{-ik(t+d_2)+i\arg T_{n1}^{21}(k)} dk \approx \mathrm{const}\cdot v_1^\phi\left(0, t\right) \exp\left(iA_n\right).$$

The functions $u_n^\phi\left(z, t\right)$ and $v_1^\phi\left(z, t\right)$ are real-valued. Hence, the magnitudes of A_n which determine phase characteristics of the step as such in the waveguides cross-section (i.e., of the transitional section of total length $d_2 \to 0$) should be a multiple of π.

The results of analysis of the short-arm junction (see Fig. 1(d) and Fig. 2: $d_1 = 0.025$ and $d_2 = 0.05$) conform the above conclusions. For the case, the functions $\arg T_{11}^{21}\left(k\right)$ and $\arg T_{31}^{21}\left(k\right)$ are coincident. The difference $\arg T_{11}^{21}\left(k\right) - \arg T_{21}^{21}\left(k\right)$ is approximately equal to π. By extrapolating the dependence $\arg T_{11}^{21}\left(k\right) \approx 0.049k + A_1$ to the range of small k's we arrive at the approximate value $A_1 \approx -0.07$. The envelopes of the E_ϕ field components of the first three transmitted waves fully coincide with the envelope of the incident pulsed wave, while that of the TE_{02}-wave is of an opposite sign. This is what is called the mode splitting effect. In essence the energy brought to the structure by a super-broadband pulse is shared between principal modes of the transmitted pulsed wave which practically replicate the primary signal structure (see Fig. 2).

Similar conclusions can be made with respect to the transmission factors $\left[T_{n1}^{21}\right]_\rho\left(k\right) = -\left[\left(k^2 - k_{n2}^2\right)\big/\left(k^2 - k_{11}^2\right)\right]^{1/2} T_{n1}^{21}\left(k\right)$ in the H_ρ-field component (the value $\left[\left(k^2 - k_{n2}^2\right)\big/\left(k^2 - k_{11}^2\right)\right]^{1/2} \to 1$ tend to one as k increases), and hence with respect to the amplitudes $v_1^\rho\left(0, t\right)$ and $u_n^\rho\left(d_2, t+d_2\right)$. An example is shown in Fig. 3 (the geometrical parameters of the junction are the same as in Fig. 1).
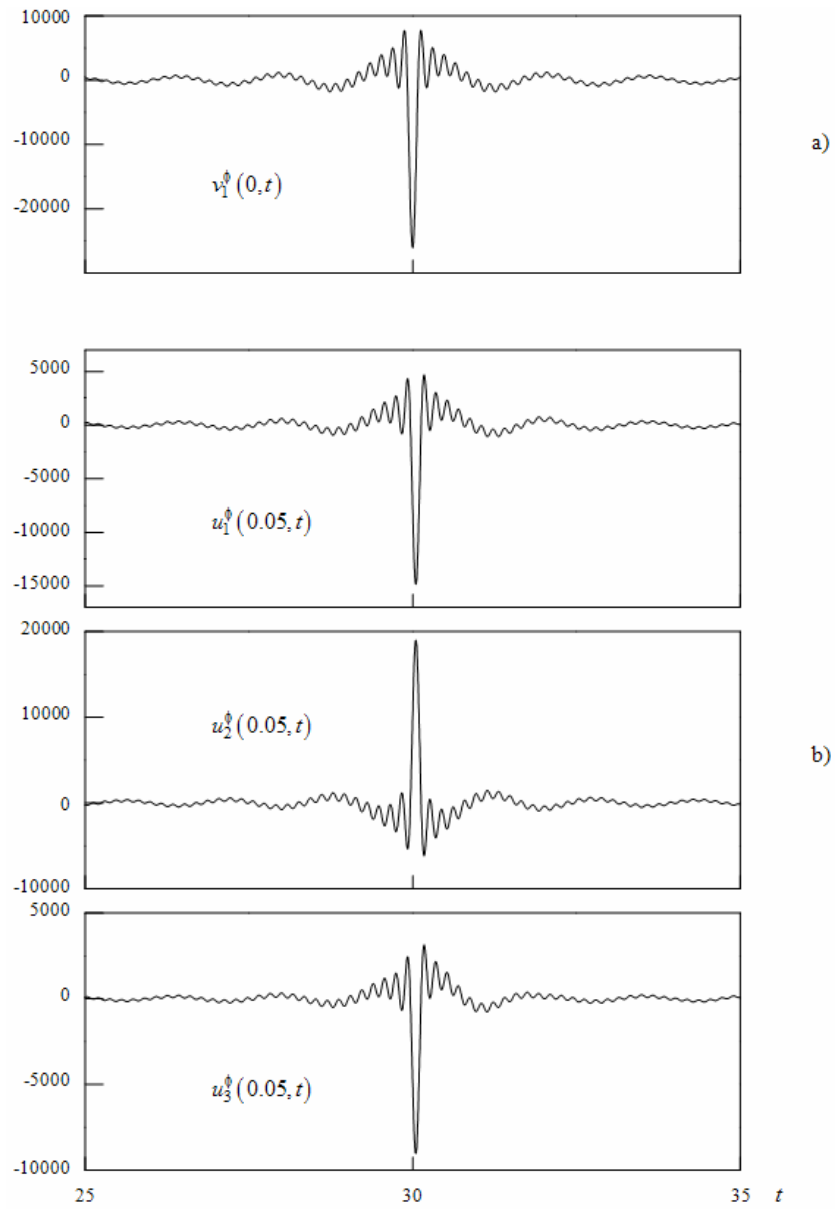
FIGURE 2. E_ϕ-component amplitudes of the super-broadband TE_{01}-pulse at the entrance to a waveguide section with the short arms (a); pulsed wave amplitudes at the section output (b).

Here the pulsed TE_{01}-wave $U^i(g,t)$ with $v_1^\rho(0,t) = F_1(t)$; $\tilde{k} = 30$, $\Delta k = 10$, $\tilde{T} = 20$, and $T = 50$ (see Fig. 3(a)), and the pulsed TE_{01}-wave

1420

$$U^i(g,t) \quad \text{with} \quad v_0^\rho(0,t) = e^{-(t-\tilde{T})^2/4\tilde{\alpha}^2} \cos\left(\tilde{k}(t-\tilde{T})\right)\chi(T-t) \; ; \quad \tilde{k}=30 \; ,$$

$\tilde{\alpha}=0.22$, $\tilde{T}=1$, and $T=12$ (see Fig. 3(b)) excite the step junction from the side of its narrower waveguide. These pulses occupy the frequency range $20 < k < 40$, with the wider and narrower waveguides being 23-M ($k > 39.92$) and 12-M ($k > 38.48$) structures, respectively, at the end of the range. The changes in the pulse waveforms at the exit from the unit are better pronounced as compared with the case of Fig. 2, because effect of the long arms of the junction where different spectral components of the signal, are characterized by different phase velocities.
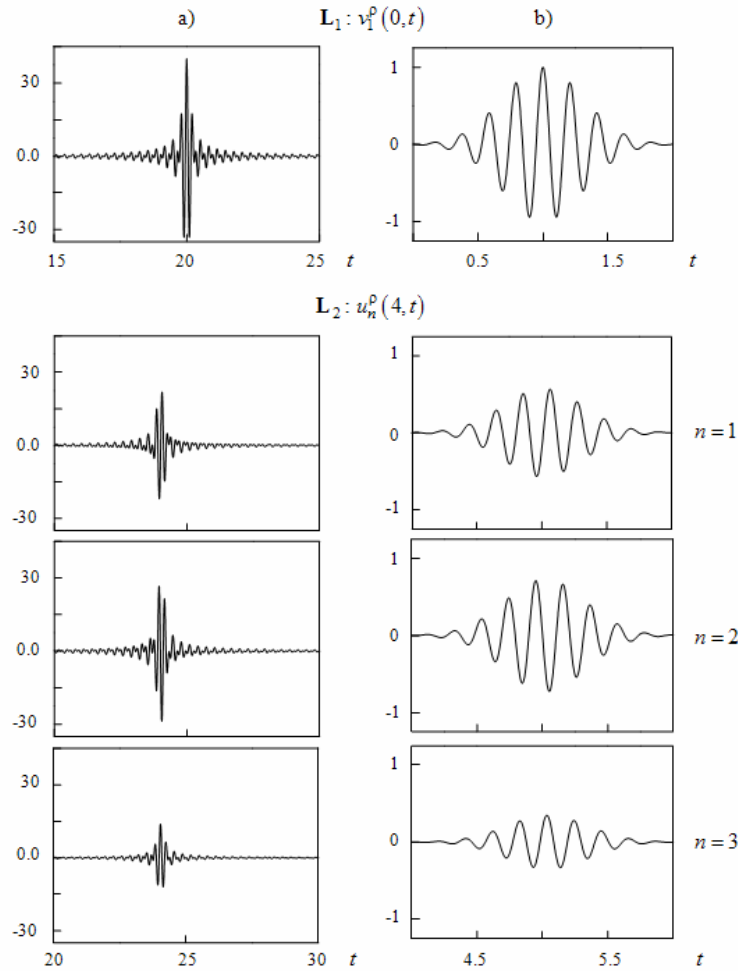
FIGURE 3. Mode splitting of super-broadband TE_{01}-pulses exciting a "narrow-to-wide" step junction in waveguides ($d_1 = 2.0$ and $d_2 = 4.0$).
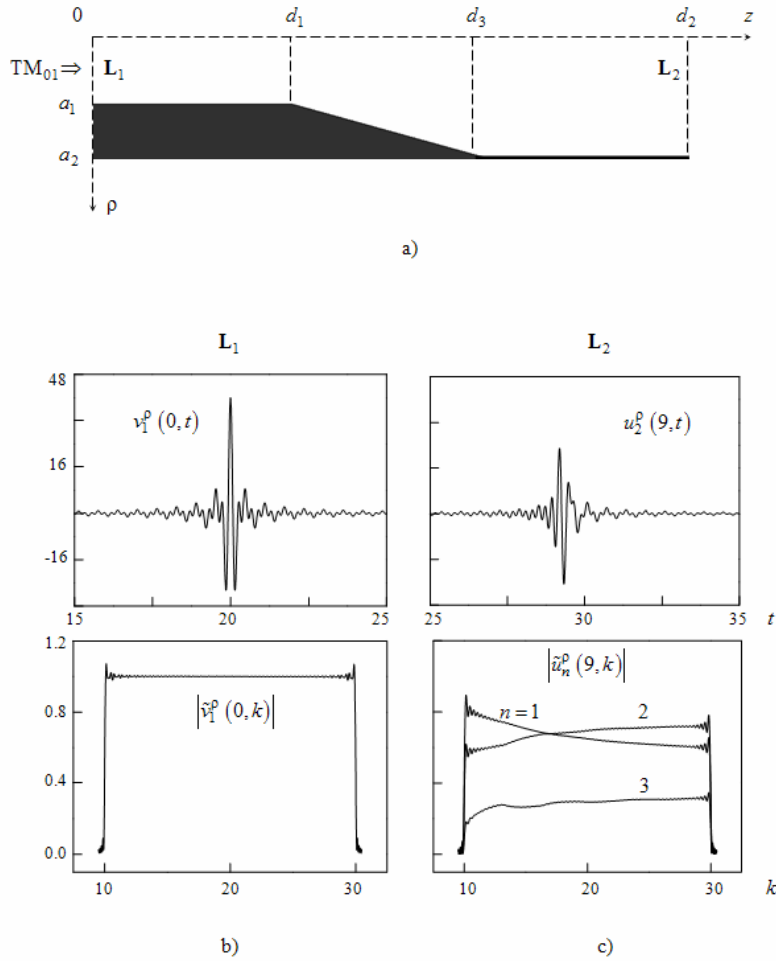
FIGURE 4. Time-domain and spectral-domain amplitudes of the transmitted waves (c) in the case of excitation of a tapered junction ((a) $a_1 = 1$, $a_2 = 1.83$, $d_1 = 3$, $d_2 = 9$ and $d_3 = 6$) by a pulsed TE_{01}-wave ((b) $U^i(g,t)$: $v_1^\rho(0,t) = F_1(t)$; $\tilde{k} = 20$, $\Delta k = 10$, $\tilde{T} = 20$, and $T = 50$) incident from the narrower waveguide.

The $\left| T_{np}^{21}(k) \right|$ dependences shown for a few first modes propagating through the wider waveguide may prove practically saturated for sufficiently great k's, even in the case of TE_{01}-mode excitation of long tapered (see Fig. 4) or smoothed (see Fig. 5(b)) junctions, as well as in the case of circular coaxial waveguide junctions excited by the TEM-mode (see Fig. 5(c)). These are also the situations where the mode splitting effect can manifest itself for the pulses

(see Fig. 5) occupying a frequency range $K_1 < k < K_2$, such that $\left| T_{np}^{21}(k) \right| \approx \text{const}(n)$ for all k's within. The shorter junctions have the smaller admissible value of parameters K_1 (see Figs. 2 and 4). Meanwhile, the junctions of long and smooth geometry excited from the narrow waveguide are characterized by smoother $T_{np}^{21}(k)$ characteristics throughout the (K_1, K_2) band and hence can provide a better replication of the primary pulse waveform in the waves propagating through the wider waveguide.
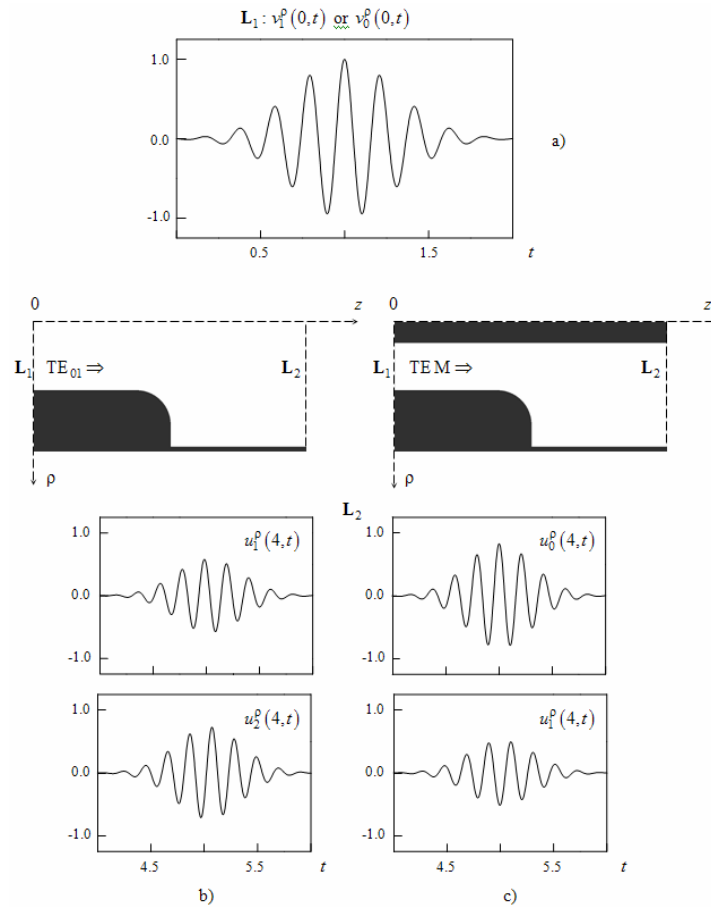
FIGURE 5. Amplitudes of the TE_{01} - and *TEM* pulsed waves (a) exciting smoothed step junctions. Amplitudes of the principal wider waveguide modes in the case of TE_{01} - and TM_{0n} - waves ((b) and (c), respectively). The basic geometrical parameters of the junctions are the same as for the junction of Fig. 1. The radius of the step rounding is equal to 0.5. The radius of the internal conductor of the coaxial waveguides is 0.3.

1423

CONICAL PLUGS IN CIRCULAR AND COAXIAL WAVEGUIDES: MODE-FREQUENCY SPLITTING OF SUPER-BROADBAND SIGNALS

The effect of strong conversion of the sinusoidal H_{10}-mode onto H_{n0}-modes ($n>1$) provoked by tilted H-plane plugs of rectangular waveguides [1] consists of special variation of the relative share of energy, $W_{n1}^{11}(k)$, carried by the H_{n0}-mode in a structure excited by the H_{10}-mode.
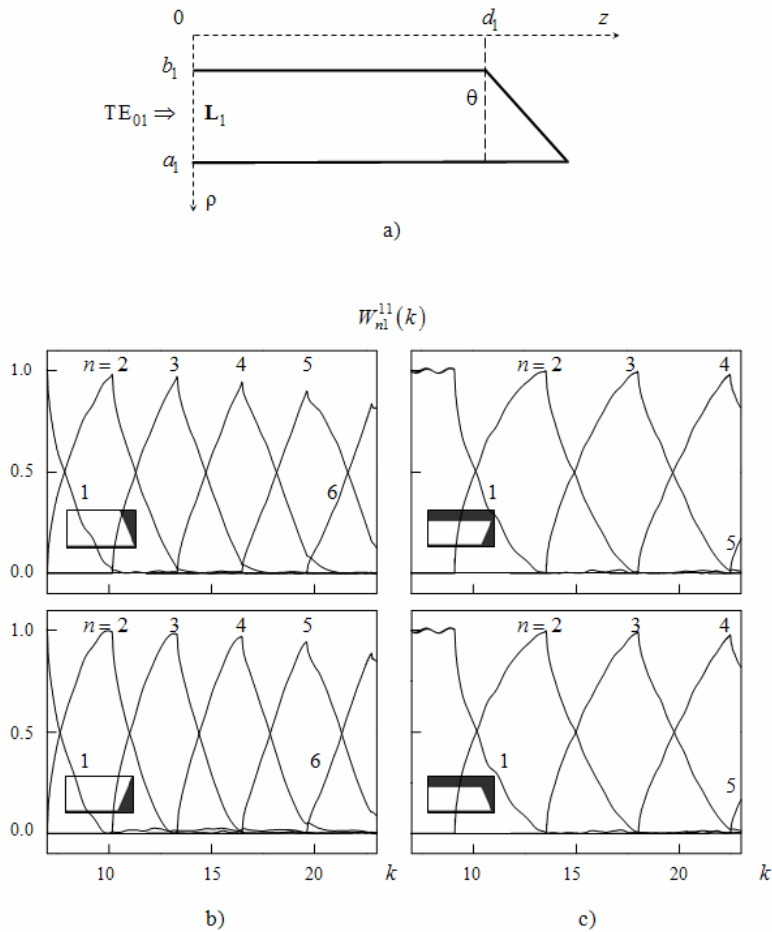
FIGURE 6. Transformation of a pulsed TE_{01}-mode ($U^i(g,t): v_1^\rho(0,t)=F_1(t);\ \tilde{k}=15,$ $\Delta k=9,\ \tilde{T}=25$, and $T=120$) by conic plugs ((a) $a_1=1,\ d_1=2$, and $\theta=120^0$; the axis of the structure symmetry is oriented along the z-axis) in a circular (b) and coaxial circular ((b) $b_1=0.3$ waveguides.
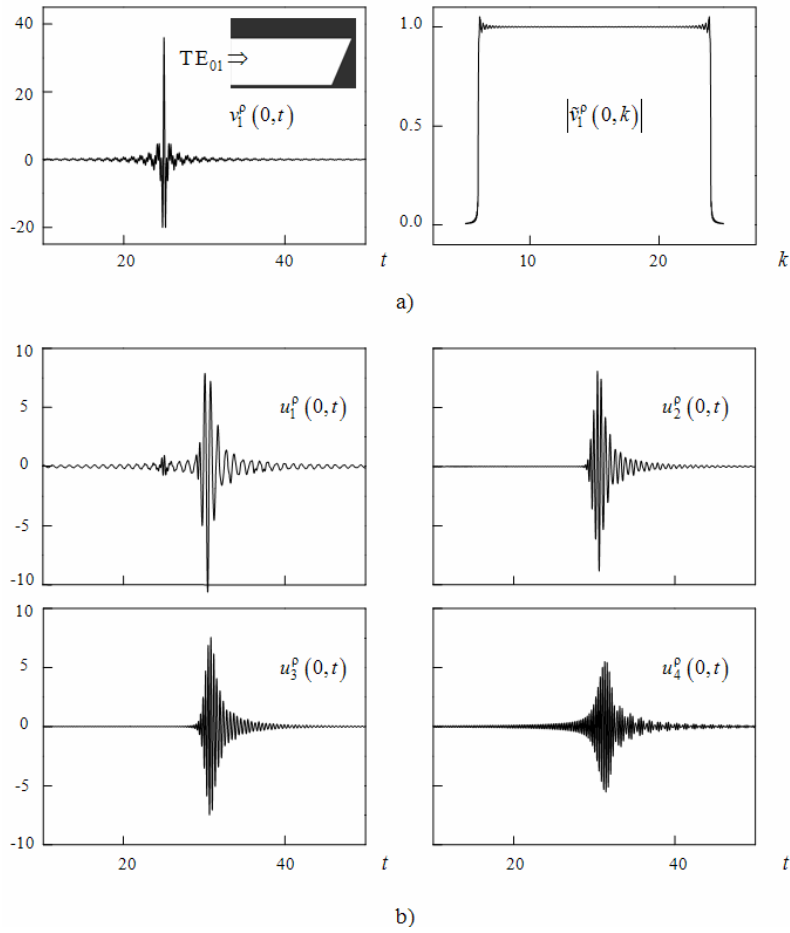
FIGURE 7. The frequency-modal splitting of a super-broadband TE_{01} pulse by a conic plug in a coaxial circular waveguide (see Fig. 6(c)). Time-domain and spectral-domain amplitudes of the primary pulse (a) and time-domain amplitudes of the reflected pulsed TE_{0n} -modes (b).

The energy shows firstly a monotonic increase within the frequency range $k_{21} < k < k_{N1}$ (k_{n1} is the cutoff frequency of the H_{n0} -mode) from the zero value at $k = k_{n1}$ to $\max_k W_{n1}^{11}(k) = W_{n1}^{11}(k_{n+1}) \approx 1$, and then decreases monotonically to $W_{n1}^{11}(k_{n+2}) << 1$. In the case of super-broadband signals the effect appears as follows. When reflected from the plug, a pulsed H_{10} -wave with spectral amplitudes uniformly distributed over the frequency range $k_{21} < k < k_{N1}$, gives rise to a set of pulsed H_{n0} -waves with $n = 2, ..., N - 2$.

1425

Each of these occupies its own spectral band $k_{n1} < k < k_{n+2,1}$. The amplitude center $\tilde{k}_n$ of the reflected H_{n0}-pulse (i.e., the central frequency of the pulse) lies at $k \approx k_{n+1,1}$ in the spectral domain.
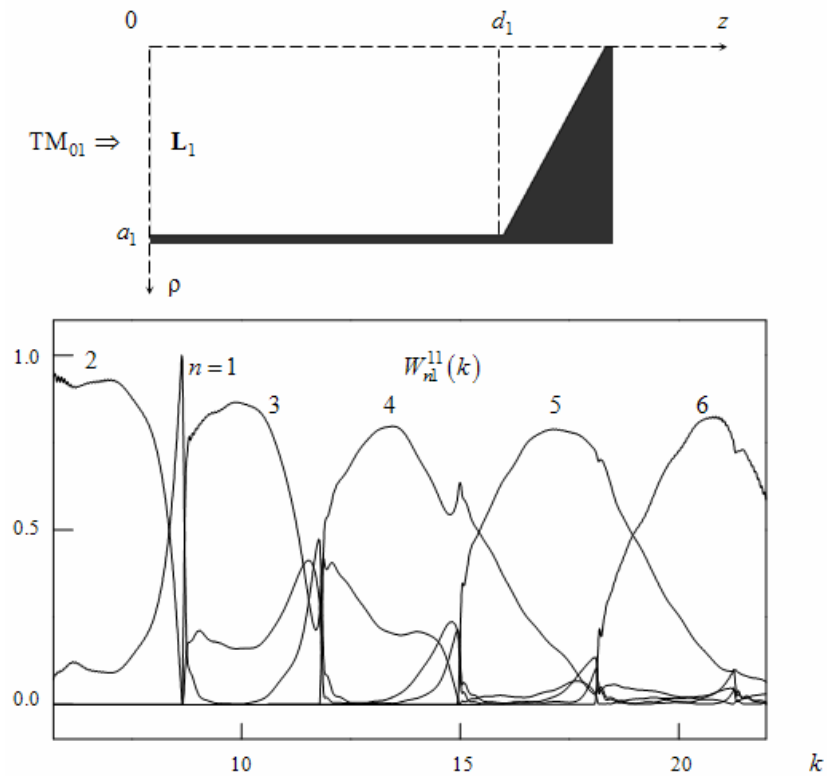
FIGURE 8. Transformation of a pulsed TM_{01}-mode ($U^i(g,t): v_1^\rho(0,t) = F_1(t)$; $\tilde{k} = 13.5$, $\Delta k = 9$, $\tilde{T} = 25$, and $T = 120$) by a conic plug in a circular waveguide ($a_1 = 1$, $d_1 = 2$, and $\theta = 120^0$).

As it occurs similar effects may accompany the scattering of super-broadband TE_{01}-pulses by conic plugs in circular and coaxial waveguides (see Figs. 6 and 7, where $\theta > 90°$ is the obtuse angle of the plug base). The effect observed may the termed the frequency-and-modal signal splitting. Essentially, a super-broadband pulse of one type (TE_{01}-mode) is converted into an ordered train of narrow-band pulses of different types (TE_{0n}-modes, with $n \geq 2$). The frequency bands occupied by each of the reflected TE_{0n} pulse, as well as the

1426

distributions of $W_{n1}^{11}(k)$ values over these bands, remain roughly the same as in the case of the H_{n0}-waves of the rectangular waveguide. The reflected TE_{0n}-pulse with a great value of n is characterized by a great value of the central frequency, $\tilde{k}_n \approx k_{n+1,1}$. This is the reason for the difference shown by oscillations of the space-time amplitudes $u_n^{\rho}(z,t)$ as functions of time t (see Fig. 7).

An effective frequency-modal splitting of the pulsed TM_{0n}-waves is impeded by the threshold effects (Wood anomalies) in the vicinity of several first slip points (cutoff points) $k = k_{n1}$ (see, for example, Fig. 8: $k_{31} \approx 8.65$, and $k_{41} \approx 11.79$). The intensity of these anomalies is much higher in the case of TM_0-modes than in the case of TE_0-waves [1-3,5-7]. For this reason, in the situation presented in Fig. 8 the reflected pulses with spectral characteristics corresponding to the frequency-modal splitting effect are not framed before the point $k = k_{51} \approx 14.93$ which is the cutoff point for the monochromatic TM_{05}-wave. However, none of these pulses show a maximum value of the power characteristic $W_{n1}^{11}(k)$ greater than 0.9.

CONCLUSIONS

Each mode propagating through a regular waveguide is characterized by its own group velocity, i.e., the motion velocity of the main body of the respective pulse [8,9]. For this reason the effects of modal or frequency-modal splitting of super-broadband result in a time-domain splitting at sufficiently great distances from the virtual boundary $\mathbf{L}_2$.

The effects giving rise to pulsed mode splitting in the axially-symmetric structures allow forming desirable field distributions across radiating apertures. These could be used in the development of manufacturable, compact-size omnidirectional antennas for base stations of wireless communication; and pulsed wave radiators with the specified sectoral radiation patterns and time-varying antenna patterns [10,11].

REFERENCES

1. Shestopalov, V.P., Kirilenko, A.A., and Rud', L.A., (1986), *Resonance scattering of waves. Waveguide inhomogeneities*. Naukova Dumka, Kiev: 216 p. (in Russian).

2. Yashina, N.P., (1979), Electromagnetic wave scattering by certain abrupt inhomogeneities in circular waveguides. *PhD thesis*, Kharkov: 20 p. (in Russian).
3. Tsakanyan, I.S., (1993), Resonance effects in multimode metal-dielectric structures in waveguides, *PhD thesis*, Kharkov: 16 p. (in Russian).
4. Sirenko K.Yu and Sirenko Yu.K., (2005), Exact absorbing conditions in initial and boundary value problems of the theory of open waveguide based resonators*, Zh. Vychisl. Matematiki and Matemat. Fiziki.* **45**(3):509-525 (in Russian).
5. Shestopalov, V.P., Kirilenko, A.A., and Masalov, S.A., (1984), *Convolution-type matrix equations in the theory of diffraction*, Naukova Dumka, Kiev: 293 p. (in Russian).
6. Shestopalov, V.P., Kirilenko, A.A., Masalov, S.A., and Sirenko, Yu.K., (1986), *Resonance scattering of waves. Diffractional gratings*, Naukova Dumka, Kiev:232p.(in Russian).
7. Rud', L.A., (1989), Free iscukkations and resonance phenomena in waveguiding structures, *Doctoral thesis*, Kharkov: 40 p. (in Russian).
8. Sirenko, Yu.K., (2003), *Transient processes in periodic, waveguide-based and compactsize open resonators: Modeling and analysis*, EDENA, Kharkov: 364 p. (in Russian).
9. Perov, A.O., Sirenko, Yu.K., and Yashina, N.P., (2004), Periodic open resonators: peculiarities of pulse scattering and spectral features, *Progress in Electromagnetics Research*. 46:33-75.
10. Brachat, P., (1994), Sectoral pattern synthesis with primary feeds, *IEEE Trans. on AP.* **42**(4):484-491.
11. Sirenko, K.Yu. and Pazynin, V.L., (2006), Axially-symmetric radiators of pulsed and monochromatic TE_{0n} - and TM_{0n} -waves, *Uspekhi sovremennoy radioelektroniki*. 4:52-69 (in Russian).